

*Supporting Information for*

# Surface morphology-dependent photoelectrochemical properties of one-dimensional Si nanostructure arrays prepared by chemical etching

*Shao-long Wu,<sup>†</sup> Long Wen,<sup>‡</sup> Guo-an Cheng,<sup>†\*</sup> Rui-ting Zheng<sup>†</sup> and Xiao-ling Wu<sup>†</sup>*

<sup>†</sup>Key Laboratory of Beam Technology and Material Modification of Ministry of Education, College of Nuclear Science and Technology, Beijing Normal University, Beijing 100875, China

<sup>‡</sup>Key Laboratory of Material Physics, Institute of Solid State Physics, Chinese Academy of Sciences, Hefei 230031, China

\*Author to whom correspondence should be addressed. E-mail: gacheng@bnu.edu.cn

Tel & Fax: +86-010-62205403

**Overview** This document contains typical cross-sectional SEM images and EDX spectra and of the 1DSiNSAs (one-dimensional Si nanostructure arrays) before and after removing of AgNPs (Ag nanoparticles), detailed structures, sizes and photogeneration profiles of the simulated nanowire device and the Si film device. And all the main optoelectronic parameters used in the simulations are listed in a table.

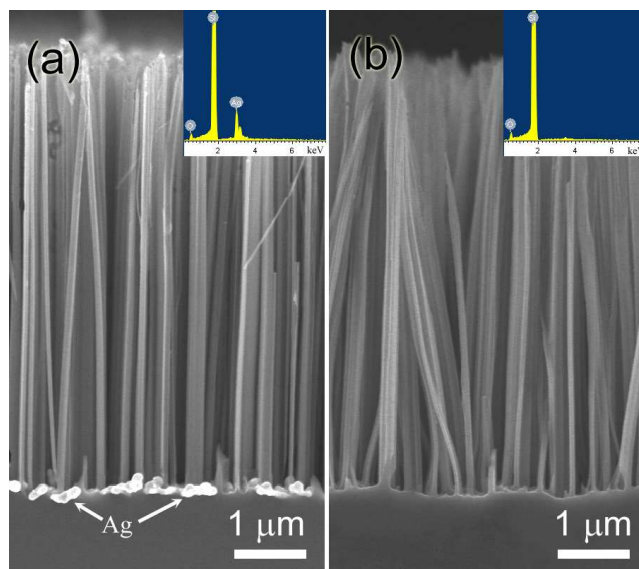


**Figure S1.** Typical cross-sectional SEM images of the 1DSiNSAs before (a) and after (b) removing of AgNPs. The insets provide the corresponding EDX spectra. Before removing treatments, numbers of AgNPs are obviously observed at the bottom of 1DSiNSAs; while after HNO<sub>3</sub> treatments, no AgNPs are observed. EDX spectra identify that the Ag elements are completely removed after the treatments. Therefore, we believe the metal ionic contamination from metal-assisted chemical etching can be ignored.

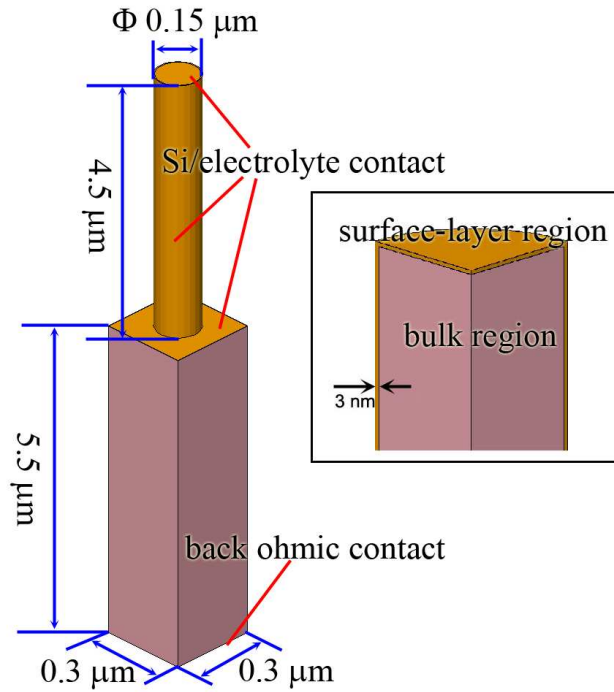


**Figure S2.** Schematic illustration of the simulated wire-array unit cell. The periodic nanowires were located on a 5.5- $\mu\text{m}$ -thick Si film, with a diameter of 0.15  $\mu\text{m}$  and a length of 4.5  $\mu\text{m}$ . The back of the substrate was set to be an ideal ohmic contact, and the surfaces of the nanowires and top-surfaces of the substrate (excluding the nanowire/substrate interfaces) was set to be the Si/electrolyte contact, approximated as a Schottky contact with an interfacial equilibrium barrier height of 1 eV. The inset shows that a surface layer with the thickness of 3 nm was added to model the effects of surface recombination on the resulting current vs. voltage characterizations. The surface-layer region possessed a different carrier lifetime from the bulk region.

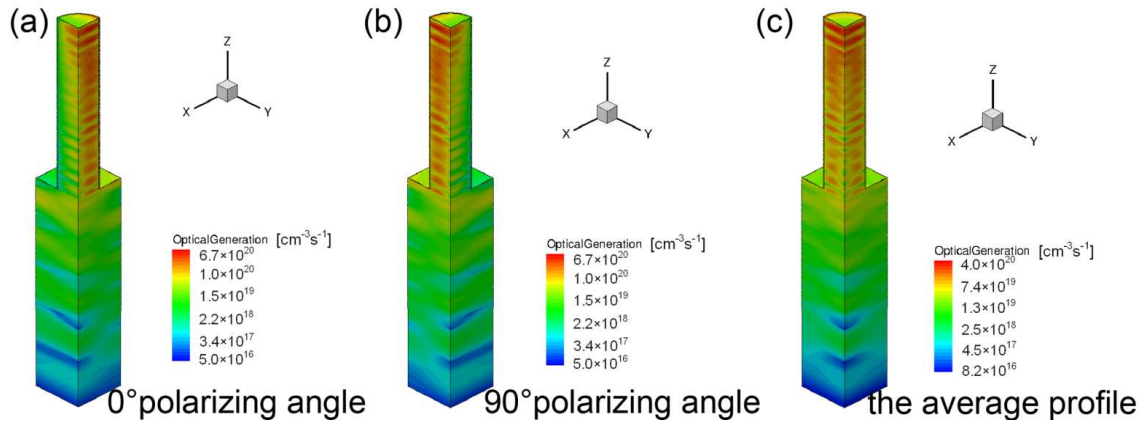


**Figure S3.** The photogeneration profiles calculated by finite-difference time-domain (FDTD) simulations under the 590-nm-wavelength light irradiation with a power density of 41.75 Wm<sup>-2</sup> and a polarizing angle of 0° (a) and 90° (b), respectively. (c) The final photogeneration profile used in the device calculations was a result of the average of the incident light with polarizing angles of 0° and 90°, to simulate the unpolarized incident light. The incident light was along the -z direction.

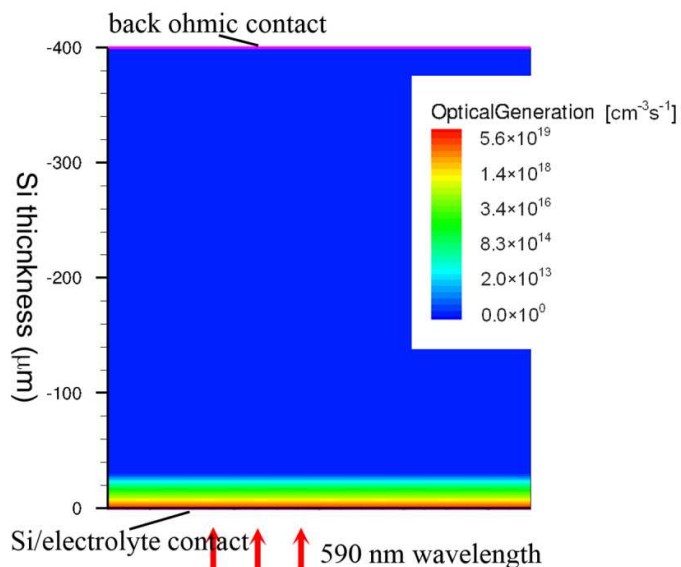


**Figure S4.** Schematic illustration of the simulated film device, and the corresponding photogeneration profile calculated by the Beer-Lambert law. The film device was simulated in a 2D model, with the thickness of 400  $\mu\text{m}$ . The back of the film was set to be a perfect ohmic contact, and the front surface was contacted by the electrolyte, approximated as a Schottky contact with an interfacial equilibrium barrier height of 1 eV. The 590-nm-wavelength light with power density of  $41.75 \text{ Wm}^{-2}$  passed through the electrolyte and then irradiated the front surface. The photogeneration profile shows that most of all the incident optical power was absorbed by the upper 25- $\mu\text{m}$ -thick layer, which can be ascribed to the relative large optical absorptivity. The lower layer was just served as the substrate and the collection layer of majority carrier, and can be worked as optical absorption layer for the long wavelength light.

**Table S1. Simulation parameters for Figure. 6b**

Parameter	Value	Units
Nanowire length	4.5	$\mu\text{m}$
Nanowire diameter	0.15	$\mu\text{m}$
Substrate thickness	5.5	$\mu\text{m}$
Barrier height	1.0	eV
Band gap	1.12416	eV
Electron affinity	4.07274	eV
Temperature	300	K
Si dielectric constant	11.7	
Doping concentration	$2.34 \times 10^{15}$	$\text{cm}^{-3}$
Intrinsic carrier density	$1.075 \times 10^{10}$	$\text{cm}^{-3}$
Effective density of states in conduction band	$2.85665 \times 10^{19}$	$\text{cm}^{-3}$
Effective density of states in valence band	$3.10463 \times 10^{19}$	$\text{cm}^{-3}$
Electron contact velocity	100	$\text{cm s}^{-1}$
Hole contact velocity	100	$\text{cm s}^{-1}$
Electron mobility	16.9725	$\text{cm}^2\text{V}^{-1}\text{s}^{-1}$
Hole mobility	4.5338	$\text{cm}^2\text{V}^{-1}\text{s}^{-1}$
Bulk electron lifetime	$1.68 \times 10^{-6}$	s
Bulk hole lifetime	$1.68 \times 10^{-6}$	s
Surface electron lifetime	$1.68 \times 10^{-10}$ - $1.68 \times 10^{-6}$	s
Surface hole lifetime	$1.68 \times 10^{-10}$ - $1.68 \times 10^{-6}$	s
Auger recombination coefficient for electron	$6.7 \times 10^{-32}$	$\text{cm}^6\text{s}^{-1}$
Auger recombination coefficient for hole	$7.2 \times 10^{-32}$	$\text{cm}^6\text{s}^{-1}$
Incident light wavelength	590	nm
Incident irradiation power density	41.75	$\text{Wm}^{-2}$
Si absorptivity at 590 nm	6385.30061	$\text{cm}^{-1}$